XXIII SIMPÓSIO BRASILEIRO DE RECURSOS HIDRÍCOS

REMOTE SENSING AND GIS BASED ANALYSIS OF GROUNDWATER DEPENDENT ECOSYSTEMS IN THE BRAZILIAN CERRADO

Rafael Barbedo Fontana[1] *& Walter Collischonn* [1]

ABSTRACT– Groundwater availability is one of the controls of vegetation distribution across regions with relatively long dry periods. In this study, a geographic information system (GIS) based modelling of the terrain was made to delineate zones with high probability of hosting groundwater dependent ecosystems. The height above nearest drainage (HAND) algorithm was applied from the digital elevation model (DEM) in a region in the Brazilian savanna, and remote sensing analyses of the vegetation was analyzed to capture its behavior. Normalized difference vegetation index (NDVI), normalized difference water index (NDWI) and energy balance evapotranspiration (ET) estimation were analyzed against the HAND. It was observed that where the probability of groundwater dependent ecosystem (GDE) occurrence was greater, vegetation had a more heterogeneous response and larger indices of greenness, humidity, and ET rate. These groundwater sensitive zones can, therefore, have important roles in water balance components, and their inclusion in hydrologic and land surface models should be taken into account.

Keywords – Remote Sensing; GDEs.

INTRODUCTION

Groundwater is of great importance in hydrological and ecological processes, such as: providing wetness or water-logged environments; preventing activation of acid sulphate soil; maintaining hydraulic gradient for groundwater discharge; sustaining water uptake by vegetation; sustaining groundwater discharge to springs; sustaining above ground wetness; sustaining base flow; preventing salt water intrusion in coastal environments; and maintaining suitable chemical composition in water supply and living environments. A groundwater dependent ecosystem (GDE) can be any ecological set that relies on substantial expressions of groundwater to maintain its functioning. A classification system of GDEs was proposed by Eamus and Froend (2006):

(I) Aquifer and cave ecosystems – including hyporheic zones of rivers and floodplains.

1) Universidade Federal do Rio Grande do Sul

(II) Ecosystems reliant on surface expression of groundwater – namely base flow rivers, streams and wetlands.

(III) Ecosystems reliant on subsurface expression of groundwater – usually via capillary fringe within the rooting depth of vegetation.

The processes that control the occurrence and maintenance of these zones are influenced by many factors, such as topography, land cover, soil characteristics, geology and climate. Typically, these systems occur in aquifer discharge areas with shallow water table – *e.g.*, lowlands and riparian zones – in regions with a markedly dry season. They exhibit hydromorphic soils and vegetation, due to their constant wet state. Groundwater discharge occurs in form of evaporation from soil top layers, transpiration from plants and base flow to river network.

In those regions, vegetation with access to groundwater typically exhibit low seasonal variability of photosynthetic activity. Therefore, remote sensing monitoring of vegetation activity presents as a good alternative for the identification of groundwater access by vegetation. The underlying concept of the remote sensing applications for identifying GDEs is that of "green islands". This approach consists in analysing and comparing adjacent pixels in an image. If a GDE covers a significant part of one pixel and not the other, it is assumed that during dry periods the vegetation responses will diverge (Eamus et al., 2015). Key indicators of GDE identification include:

- Low variability of vegetation activity across wet and dry periods.
- Topographic depressions and breaks of slope across the catchment, derived from digital elevation models.
- Low water table depth.

Some studies have applied the above concepts in identification and analyses of GDEs, particularly in semi-arid regions across Australia, China and South Africa. Münch and Conrad (2007) used Landsat images' normalized difference vegetation index (NDVI) to classify vegetation and relate it to landscape wetness potential, slope and flow accumulation – obtained by morphological characteristics of terrain – and depth to groundwater – obtained by combining measurements of groundwater level in boreholes with digital elevation model data. The study provided a GDE probability rating map for a catchment in South Africa, concluding that remote sensing based classification combined with GIS based modelling could produce a regional-scale map of the distributions of GDEs.

A similar method was used by Tweed et al. (2007) in a south-eastern Australia catchment. They identified GDEs by mapping groundwater discharge and recharge zones. Using Landsat NDVI time series as measures of vegetation combined with topographic indices – such as profile curvature and

wetness potential – and borehole data, they generated a map of potential recharge and discharge areas at the catchment scale.

Lv et al. (2013) related NDVI with depth to groundwater in a semi-arid region in northern China. It was demonstrated that the largest and most diverse NDVI values occurred at the sallowest depths to groundwater across the 2600 km² catchment studied (Figure 1). They classified five different land cover types of GDEs and found a threshold at 10m depth, from which vegetation cover and diversity are relatively insensitive to further increments in groundwater depth.

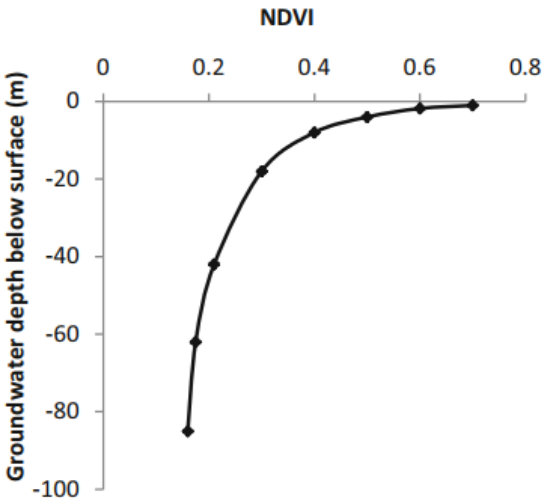

Figure 1: Relationship between NDVI and depth-to-groundwater for the Hailiutu River catchment in northern China (Eamus et al., 2016).

Several vegetation indices variations of Landsat images were used by Barron et al. (2014) in south-west Australia at the end and beginning of both 'wet' and 'dry periods to classify vegetation cover. Results were validated with 'in-situ' data on geomorphologic characteristics and evapotranspiration estimations. The study provided a practical tool for mapping GDEs in regions with well-defined seasonal rainfall.

REGION OF STUDY

The Pandeiros river is located in central Brazil (Figure 2). It is a tributary of the São Francisco river. The drainage area of the basin is about 3000 km², average annual rainfall being around 1000 mm, with rainfall concentrated from November to April (wet season). It is in a tropical climate zone, with warm temperatures ranging from 18 to 27 ºC year-round. The basin is located in the Brazilian tropical savannah, called the cerrado.

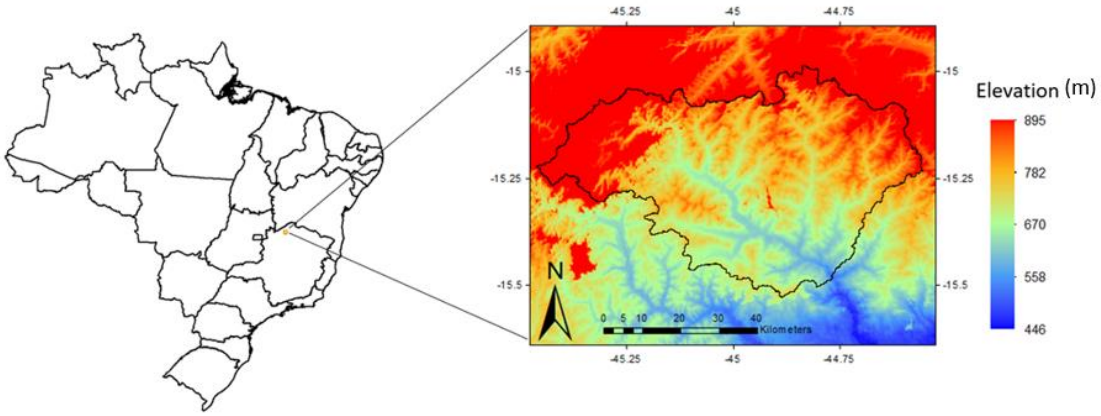

Figure 2: The Pandeiros river basin in the context of the Brazilian territory.

The vegetation is a mix of grasslands and deep-rooted trees well adapted to long dry periods. In the valley bottoms close to the drainage networks, where groundwater is close to surface, a different kind of vegetation formation locally called "vereda" occurs. This riparian vegetation lies on hydromorphic soils along river beds, with evergreen trees and shrubs moist all year round, surrounded by grasslands belts between them and the typical cerrado formations. Its hydrologic functioning is not well understood yet. It covers a small portion in the basin, but it may play an important role in water balance processes, since soil is groundwater moist all year round, and therefore supports a large portion of phreatophyte vegetation.

METHODS

Terrain processing

The Multi-Error-Removed Improved-Terrain Digital Elevation Model (MERIT DEM) product (Yamazaki et al., 2017) was used herein to derive Height Above Nearest Drainage (HAND) (Nobre et al., 2011; Rennó et al., 2008). The HAND takes DEM derived flow direction and stream definition and gives the vertical distance of a given grid point to the nearest drainage, often called draining potential. Grid points can, then, be classified accordingly to their respective draining gravitational potential, which are inferred to have similar hydrological proprieties that match with soil water and land cover characteristics.

Vegetation indices

In order to capture groundwater activity, it was taken an image at the end of the dry period, where there is little recent rainfall that could mislead the analyses. It was used a Landsat 8 image of

2015 September 23 – at the end of the dry season. Landsat sensor was chosen because of its fine spatial resolution (30m), which can better capture the vegetation activity across the landscape. Two spectral indices were derived from the image: Normalized Difference Vegetation Index (NDVI) and Normalized Difference Water Index (NDWI). NDVI and NDWI are typically used as proxies of photosynthetic activity and moisture content, respectively. They are obtained by

$$NDVI = \frac{NIR - red}{NIR + red}, \quad (1)$$

$$NDWI = \frac{NIR - SWIR}{NIR + SWIR}, \quad (2)$$

where NIR is near-infrared band, red is red band and $SWIR$ is short-wave-infrared band. NDVI values vary from 0 to 1 for vegetation, and are negative for bare soil or water. NDWI values vary from -1 to 1, where values greater than 0 indicate high vegetation moisture content.

Evapotranspiration (ET) estimation

The evapotranspiration (ET) estimation was done using the surface energy balance algorithm for land (SEBAL) (Allen et al., 2011; Bastiaanssen et al., 1998). It uses surface temperature, surface reflectance and NDVI, as well as their interrelationships to infer surface fluxes. The advantage of energy balance based over vegetation based methods is that actual ET rather than potential ET is computed – capturing ET reductions caused by stress of disease, salinity or shortage soil moisture. Disadvantage lies on the fact that it requires accurate estimations of surface fluxes, such as net radiation, soil heat and sensible heat. SEBAL attempt to overcome this disadvantage by focusing internal calibration of latent heat and sensible heat to absorb intermediate estimation errors and biases (Allen et al., 2011).

The internal calibration was performed by an automated method proposed by Allen et al. (2013). The algorithm was applied in the Google Earth Engine Platform (Gorelick et al., 2017). Climate data were obtained from the Global Land Data Assimilation System (GLDAS), which integrates satellite-based and ground-based data sets for parameterizing, forcing and constraining land surface models (Qi et al., 2015).

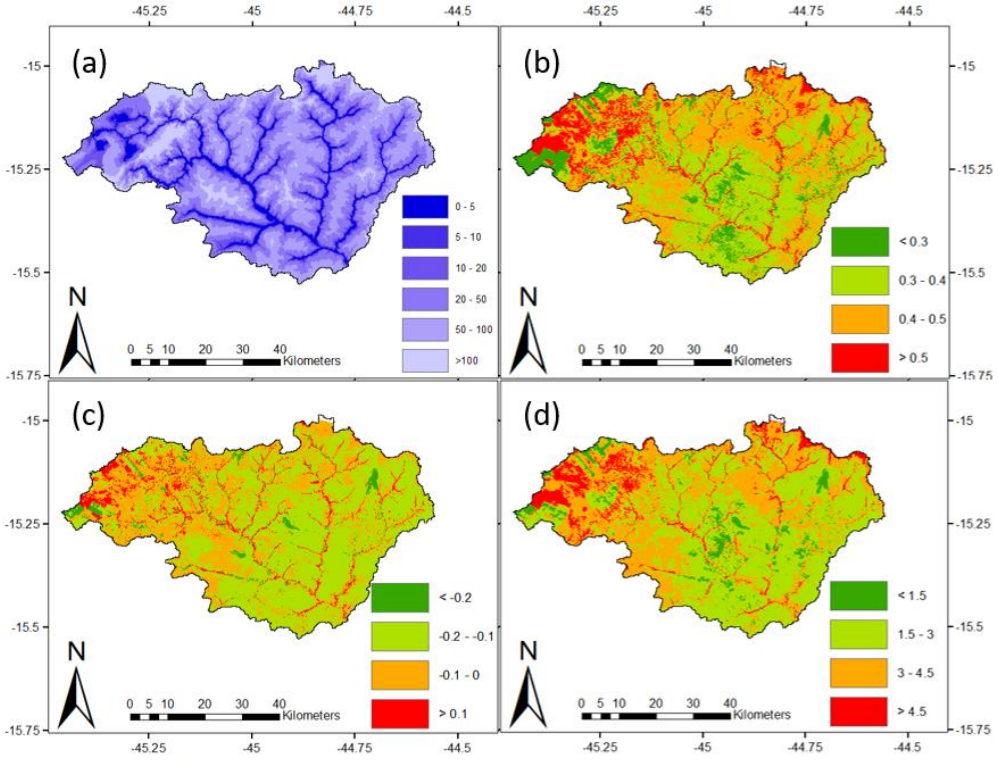

Figure 3: Metrics used in the Pandeiros river basin: (a) HAND in m, (b) NDVI, (c) NDWI, (d) daily ET in mm.

RESULTS

Distribution of spectral indices

The spectral indices were analyzed against HAND measures (Figure 4). When HAND is shallow, which indicates lower groundwater level, the distribution of both indices has a wider range of values, indicating the presence of more variety of vegetation types. As HAND goes higher, distributions become narrower, indicating a more homogeneous vegetation cover.

In order to analyze the dependency of vegetation characteristics on groundwater, mean and standard deviation of NDVI, NDWI and daily ET (in mm) were calculated with increase of HAND. It was applied 1 m intervals of HAND to group the values. The results are shown until a HAND value of 30 m, because further increases did not have a sufficiently large number of values to capture statistical characteristics. It can be seen that the mean and the standard deviation of NDVI, NDWI and ET values decreases with increasing HAND, and approximately approach constant values when HAND is greater than 15 m. They both indicate that vegetation is more active and diverse as HAND values decrease.

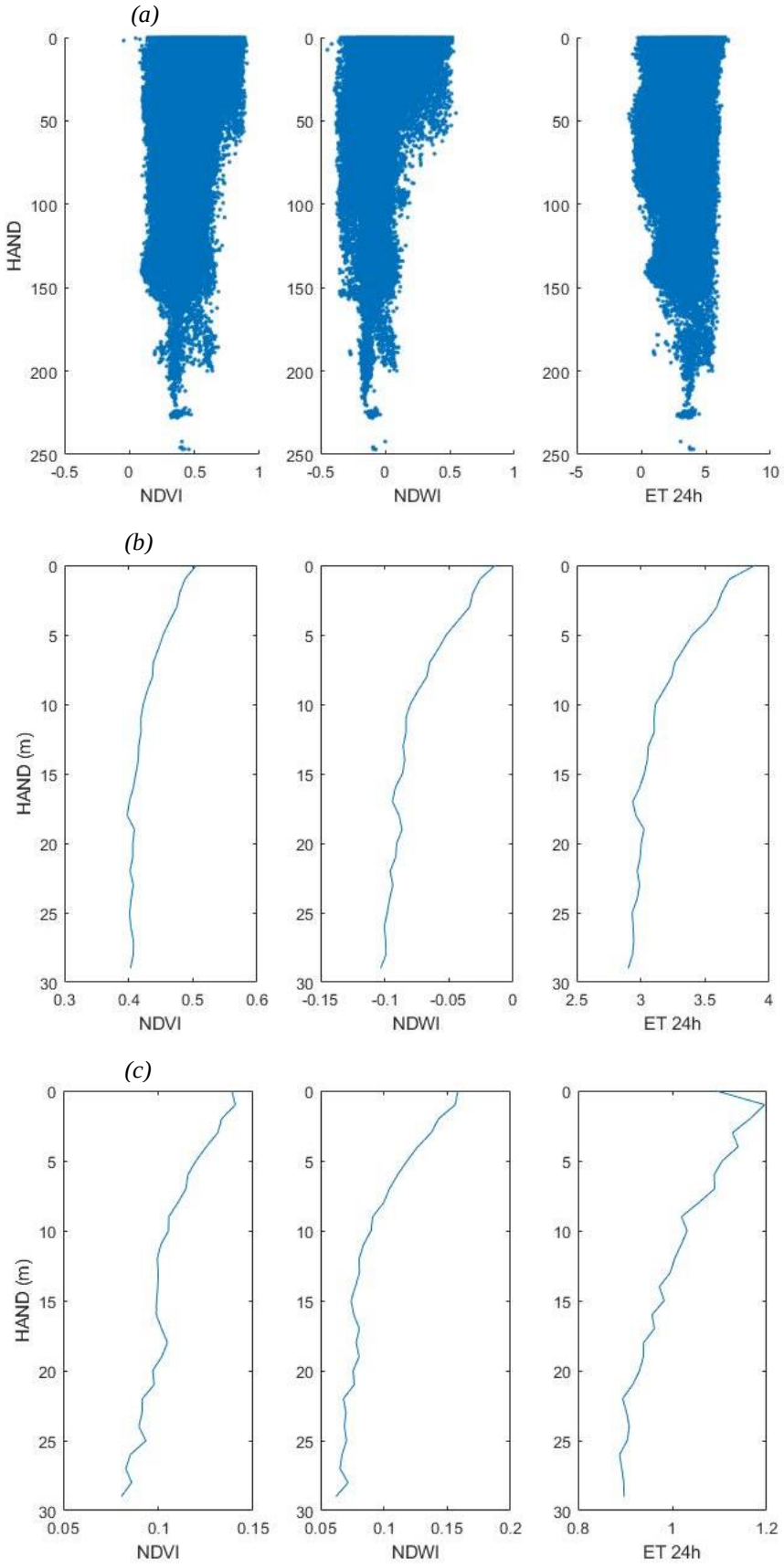

Figure 4: Scatter plots of HAND against NDVI, NDWI and ET 24h (a); mean (b) and standard deviation (c) of NDVI, NDWI and ET 24h against HAND over 1 m interval classes.

Vegetation activity

A HAND threshold of 5 m was used to classify the terrain in two categories: probably saturated and probably not saturated. The probably saturated region incorporates the riparian vegetation of cerrado, in which, as seen, have distinct response in the dry season. Within a buffer zone where HAND < 5 m (Figure 5), vegetation exhibits distinguishable characteristics. It can be seen in Table 1 that the rate of high NDVI, NDWI and ET 24h values (thresholds set to 0.5, 0.0 and 4.5, respectively) is much greater in these buffer zones than in the rest of the basin. The results indicate that in the dry season, the zone close to the stream channel have greater proportion of vegetation with high photosynthetic activity.

HAND	Area proportion	NDVI > 0.5 rate	NDWI > 0 rate	ET > 4.5 rate
< 5 m	0.069	0.407	0.309	0.277
> 5 m	0.093	0.103	0.047	0.074

Table 1: Buffer zone defined by HAND, area proportion and vegetation activity.

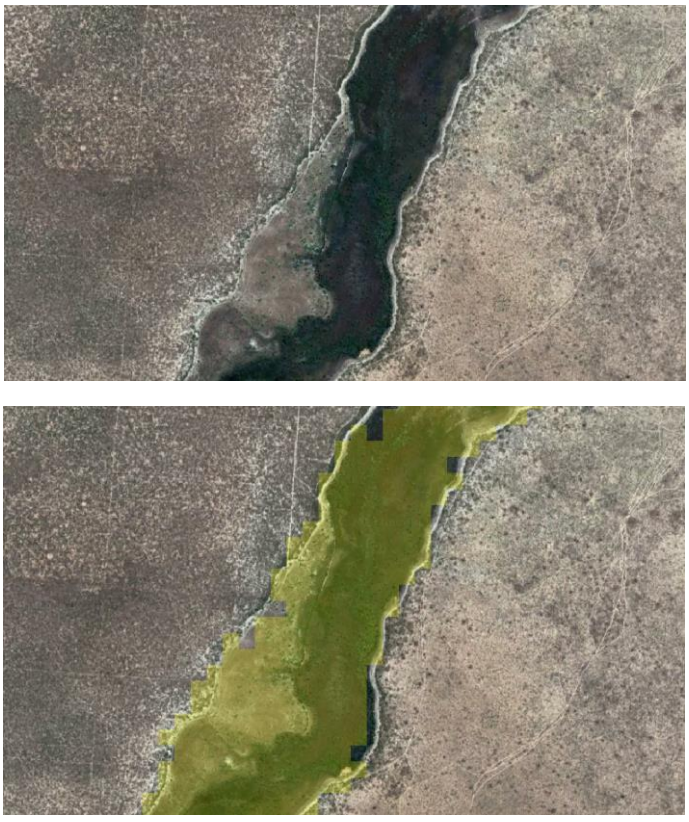

(a)

(b)

Figure 5: Satellite picture of a 'vereda', riparian zone in the cerrado (a), and buffer zone indicating HAND < 5 m.

CONCLUSION

It was made an application of the HAND algorithm and analyzed remote sensing derived vegetation measures in order to capture the behavior of GDEs. It was used a Landsat 8 image on the end of the dry season. Results show that the vegetation has more activity and diversity responses at the valley bottoms (when HAND is smaller), which coincides with other authors statements (Lv et al., 2012). When HAND < 5 m, evergreen vegetation, i.e. groundwater dependent, is more present and, consequently, evapotranspiration rates are greater.

For this analysis, it was not taken into account the anthropization occurred in the area, especially those within the buffer zone, that surely had influence on the results. Next, it could be applied a mask on farmland zones, in which groundwater dependent vegetation would be surely absent. A groundwater model with boreholes level validation would be better suited to correlate with vegetation measures, which should be considered for validating the HAND algorithm or other DEM-based algorithms in identification of zones with potential to host GDEs.

REFERENCES

Allen, R., Irmak, A., Trezza, R., Hendrickx, J.M.H., Bastiaanssen, W., and Kjaersgaard, J. (2011). Satellite-based ET estimation in agriculture using SEBAL and METRIC. Hydrological Processes *25*, 4011–4027.

Allen, R.G., Burnett, B., Kramber, W., Huntington, J., Kjaersgaard, J., Kilic, A., Kelly, C., and Trezza, R. (2013). Automated Calibration of the METRIC-Landsat Evapotranspiration Process. JAWRA Journal of the American Water Resources Association *49*, 563–576.

Barron, O.V., Emelyanova, I., Niel, T.G.V., Pollock, D., and Hodgson, G. (2014). Mapping groundwater-dependent ecosystems using remote sensing measures of vegetation and moisture dynamics. Hydrological Processes *28*, 372–385.

Bastiaanssen, W.G.M., Menenti, M., Feddes, R.A., and Holtslag, A.A.M. (1998). A remote sensing surface energy balance algorithm for land (SEBAL). 1. Formulation. Journal of Hydrology *212–213*, 198–212.

Eamus, D., and Froend, R. (2006). Groundwater-dependent ecosystems: the where, what and why of GDEs. Australian Journal of Botany *54*, 91–96.

Eamus, D., Zolfaghar, S., Villalobos-Vega, R., Cleverly, J., and Huete, A. (2015). Groundwater-dependent ecosystems: recent insights from satellite and field-based studies. Hydrology and Earth System Sciences *19*, 4229–4256.

Eamus, D., Fu, B., Springer, A.E., and Stevens, L.E. (2016). Groundwater Dependent Ecosystems: Classification, Identification Techniques and Threats. In Integrated Groundwater Management: Concepts, Approaches and Challenges, A.J. Jakeman, O. Barreteau, R.J. Hunt, J.-D. Rinaudo, and A. Ross, eds. (Cham: Springer International Publishing), pp. 313–346.

Gorelick, N., Hancher, M., Dixon, M., Ilyushchenko, S., Thau, D., and Moore, R. (2017). Google Earth Engine: Planetary-scale geospatial analysis for everyone. Remote Sensing of Environment *202*, 18–27.

Lv, J., Wang, X.-S., Zhou, Y., Qian, K., Wan, L., Eamus, D., and Tao, Z. (2012). Groundwater-dependent distribution of vegetation in Hailiutu River catchment, a semi-arid region in China. Ecohydrology *6*, 142–149.

Münch, Z., and Conrad, J. (2007). Remote sensing and GIS based determination of groundwater dependent ecosystems in the Western Cape, South Africa. Hydrogeology Journal *15*, 19–28.

Nobre, A.D., Cuartas, L.A., Hodnett, M., Rennó, C.D., Rodrigues, G., Silveira, A., Waterloo, M., and Saleska, S. (2011). Height Above the Nearest Drainage – a hydrologically relevant new terrain model. Journal of Hydrology *404*, 13–29.

Qi, W., Zhang, C., Fu, G., and Zhou, H. (2015). Global Land Data Assimilation System data assessment using a distributed biosphere hydrological model. Journal of Hydrology *528*, 652–667.

Rennó, C.D., Nobre, A.D., Cuartas, L.A., Soares, J.V., Hodnett, M.G., Tomasella, J., and Waterloo, M.J. (2008). HAND, a new terrain descriptor using SRTM-DEM: Mapping terra-firme rainforest environments in Amazonia. Remote Sensing of Environment *112*, 3469–3481.

Tweed, S.O., Leblanc, M., Webb, J.A., and Lubczynski, M.W. (2007). Remote sensing and GIS for mapping groundwater recharge and discharge areas in salinity prone catchments, southeastern Australia. Hydrogeology Journal *15*, 75–96.

Yamazaki, D., Ikeshima, D., Tawatari, R., Yamaguchi, T., O'Loughlin, F., Neal, J.C., Sampson, C.C., Kanae, S., and Bates, P.D. (2017). A high-accuracy map of global terrain elevations. Geophysical Research Letters *44*, 5844–5853.